ICSV13 - Vienna
The Thirteenth International Congress on Sound and Vibration
Vienna, Austria, July 2-6, 2006

FORCE PREDICTION VIA THE INVERSE FRF USING EXPERIMENTAL AND NUMERICAL DATA FROM A DEMONSTRATOR WITH TUNEABLE NONLINEARITIES

Ekke J. Oosterhuis*, Wouter B. Eidhof, Peter J.M. van der Hoogt and André de Boer

Chair of Structural Dynamics and Acoustics, University of Twente
P.O. Box 217, 7500 AE Enschede, The Netherlands
E.J.Oosterhuis@ctw.utwente.nl

Abstract

Force prediction can basically be done by two methods: direct methods and optimization methods. Direct methods use the inverse of the forward system model to calculate the excitation directly from the measured responses. Optimization methods use a forward model in an optimization loop wherein the input to the forward model is adjusted until the model responses matches the measured responses. In practice, a direct method using an experimentally obtained Frequency Response Function (FRF) is generally used. The direct method can be applied iteratively to enable convergence towards an excitation signal when dealing with nonlinear systems. Previous research of the authors, applying such a code to a highly nonlinear multibody quarter car model, showed an acceptable match between the calculated and the original excitation. However, the iterative process takes many steps and needs user interaction to reach overall convergence, like the manual exclusion from the time signal of excitation peaks that cause divergence. The test case is a representative benchmark for real life problems. This paper focuses on the improvement of speed and robustness of force prediction methods when dealing with nonlinear systems. Contrary to commercial codes, where the system model is treated as a black-box, we use a-priori knowledge of the system dynamics obtained from parametric modeling. We set out from the direct method using the inverse FRF. A simple demonstrator has been built consisting of a beam, clamped at one side and the other side subjected to different end conditions: free and supported by a repulsing magnet. The demonstrator has also been modeled in a multibody code supporting flexible bodies, to enable preliminary research and to compare experiments and simulations. This paper is restricted to the reconstruction of harmonic forces acting at known locations with different amplitudes and frequencies.

INTRODUCTION

Due to the increasing demand for light weight constructions in cars, material fatigue becomes a key design driver. In vehicle durability testing responses to road excitation are measured in real life and then replicated on a test-rig. The calculation of the excitation signals (drives) to the test-rig such that the test-rig responses equal the real life target responses, is called drive file development. One of the aims of this project is the improvement of the speed and robustness of this calculation. Drive file development is a specific case of force prediction, i.e. the calculation of excitation via known responses.

Force prediction can basically be done by two methods [1]: the *direct* method and the *optimization* method.

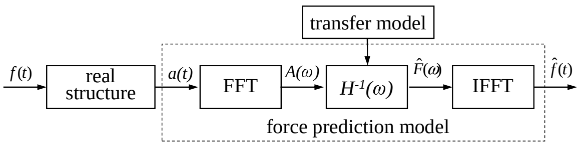

Figure 1: Direct (force prediction) method

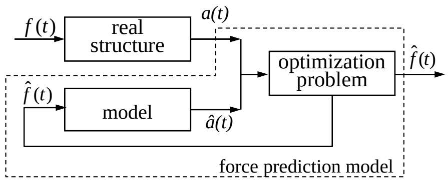

Figure 2: Optimization method

Direct methods use the inverse of the forward system model to calculate the excitation directly from the measured responses, c.f. fig. 1. Optimization methods use a forward model in an optimization loop where the input to the forward model is adjusted until the model responses match the measured responses; the model input is then assumed to equal the original excitation, c.f. fig. 2. Most force prediction methods are direct methods, see e.g. [2]. In general, a shift is going on from methods in the frequency domain towards the time domain [3]. Main reason for this is the inability to capture very time limited events in the frequency domain. These events play an important role in exciting nonlinearities. Few attempts have been made to force prediction on strongly nonlinear systems e.g. [4]. For these problems the optimization methods seem most suited.

Mainly due to the ease of and experience with frequency domain system identification, commercial drive file development codes used in the automotive industry apply the direct method with a FRF system model. To avoid over-excitation and thus probable damage when dealing with nonlinear systems, the direct method is applied iteratively, cautiously updating the excitation.

To gain insight in the effects of applying a direct method to a nonlinear system when dealing with non-periodic responses, we examine a simple demonstrator. The demonstrator consists of a beam, clamped at one end and at the other end free (linear case) or with a repulsing magnet (nonlinear case). Force prediction is an inherently ill-posed problem, i.e. there is no unique solution, unless a-priori information is provided. We therefore assume the location where the unknown force acts to be known. We restrict ourselves to the reconstruction of harmonic excitations in this paper.

LINEAR DEMONSTRATOR: CLAMPED-FREE BEAM

The linear demonstrator consists of a clamped-free aluminium beam with dimensions as in fig. 3, equipped with four accelerometers and excited by shakers via stingers to ensure excitation normal to the beam. The force transducers are mounted directly to the beam. The magnets shown in this figure are not part of the linear demonstrator.

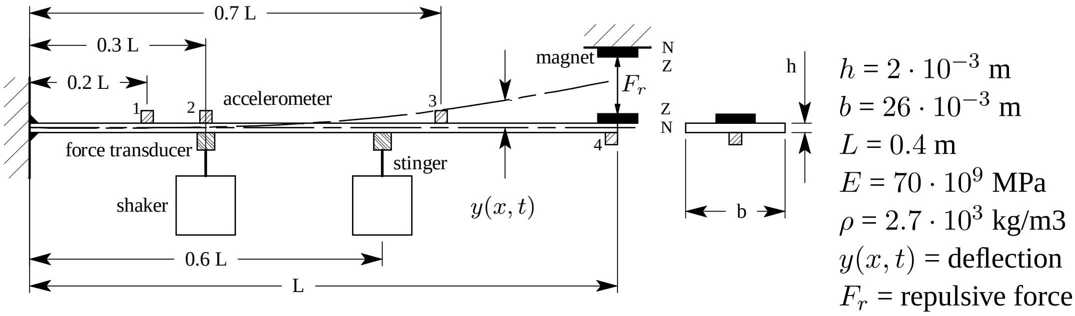

Figure 3: Demonstrator beam

Analytical and experimental FRFs

The FRF$_{kl}$ between accelerations $A_l(\omega)$ measured at position x_l and a harmonic force $F_k(\omega)$ at position x_k is given by [5]:

$$FRF_{kl}(x_l, x_k) = \frac{A_l(x_l)}{F_k(x_k)} = -\omega^2 \sum_r \frac{\varphi_r(x_l)\varphi_r(x_k)}{(-\omega^2 + \omega_r^2) + j2\omega\omega_r\zeta_r} \tag{1}$$

Where ω is the angular excitation frequency, ω_r the r^{th} angular eigenfrequency, φ_r the r^{th} normal mode, j the imaginary unit and ζ_r the viscous damping ratio of the r^{th} mode. Only the first four modes are taken into account in the analytical FRF, restricting accurate model behavior to a frequency range up to 500 Hz. Both the analytically and experimentally derived eigenfrequencies of these modes are given in tab. 1 along with their modal damping ratios that were defined experimentally.

FRF	f_1 [Hz]	f_2 [Hz]	f_3 [Hz]	f_4 [Hz]
analytical	10.3	64.4	180.4	353.5
experimental	10.5	63.5	178.8	352.3
damping	ζ_1 [-]	ζ_1 [-]	ζ_1 [-]	ζ_1 [-]
experimental	$12 \cdot 10^{-3}$	$7 \cdot 10^{-3}$	$4 \cdot 10^{-3}$	$19 \cdot 10^{-3}$

Table 1: First four analytical and experimental eigenfrequencies and the damping ratios

Figure 4 shows the moduli of the analytically and experimentally determined FRFs for excitation at $0.3L$ to the sensors at $0.3L$ and L. The FRFs show a reasonable match in the resonances; the mismatches in the higher (anti-)resonances are mainly due to not modeling the contribution of the added mass of the sensor and shakers analytically. Also the positions of shakers and sensors will differ slightly between the experimental and analytical model. However, the degree of correspondence between the analytical and experimental FRFs is sufficient to get familiar with the pitfalls of the direct inverse method.

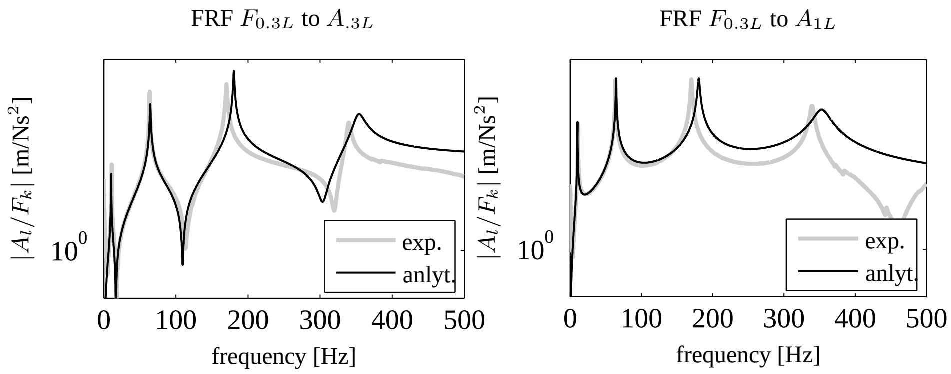

Figure 4: Analytical and experimental FRFs

To check the assumed linearity of this demonstrator, the FRF from the shaker at $0.6L$ to the sensor at L was determined at different excitation levels in the range of our interest. Figure 5 shows these FRFs along with the coherence. Since the FRFs are nearly identical and the coherence is excellent, it can be stated that the demonstrator behaves linearly in the excitation range of interest.

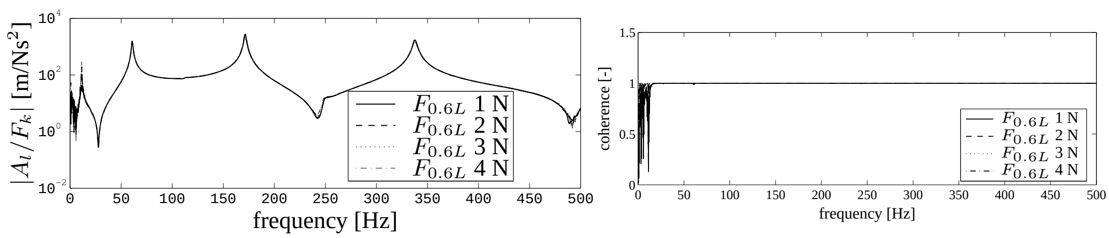

Figure 5: FRFs and coherences from excitation at 0.6L to a sensor at 1L

Force prediction

Reconstruction of the applied force is done by multiplying the responses with the inverse transfer H_{nm}. Here the transfer H_{nm} is a matrix of FRFs (FRM) from n excitations to m sensors.

$$\hat{F}_n(\omega) = H_{nm}(\omega)^{-1} A_m(\omega) \tag{2}$$

where $\hat{F}_n$ is the reconstructed force vector and A_m is the vector of accelerations responses in the frequency domain. In case of a linear analytical model and analytically derived responses this gives exact results. Using the experimentally derived transfer H_{nm} and measured responses, three main sources of error exist:

- inaccuracies in the experimentally determined FRFs
- measurement noise

- insufficient/inaccurate sensor data

It is obvious that an inaccurate model cannot lead to good force prediction results. The locations of the sensors and shakers during system identification should be exactly equal to the locations during the response measurement. Measurement noise is the main source of erratic results. The influence of noise during system identification is suppressed by using the so called $H_{1_{nm}}$ estimator:

$$H_{1_{nm}}(\omega) = \frac{S_{af}(\omega)}{S_{ff}(\omega)} = \frac{A_m(\omega)F_n^*(\omega)}{F_n^*(\omega)F_n(\omega)} \quad (3)$$

where $S_{af}(\omega)$ is the cross-spectrum between the measured accelerations $a_m(t)$ and the forces $f_n(t)$, $S_{ff}(\omega)$ is the auto-spectrum of the excitation and * denotes the complex conjugate. The use of the cross-spectrum removes uncorrelated noise between excitation and response from the transfer. However, noise can still disturb force prediction. Suppose the measured response $A_m(\omega)$ is the sum of the true response $Y_m(\omega)$ and some noise $N_m(\omega)$. Then the predicted force is given by [2]:

$$\hat{F_n}(\omega) = H_{1_{nm}}^{-1}(\omega)A_m(\omega) = H_{1_{nm}}^{-1}(\omega)Y_m(\omega) + H_{1_{nm}}^{-1}(\omega)N_m(\omega) \quad (4)$$

If $|H_1(\omega)|$ is very small at a certain frequency (as in anti-resonances, c.f. fig. 4), then $|Y(\omega)|$ is also small and hence the second term in eq. 4 becomes dominant at that frequency. The noise $N(\omega)$ is amplified by the division through the small $|H_1(\omega)|$. This is illustrated in fig. 6, where the true force F is shown together with a predicted force $\hat{F}$ using the analytical model and the corresponding analytical responses contaminated with about 10% noise. The FRF is shown to indicate the anti-resonances, e.g. at 120 Hz.

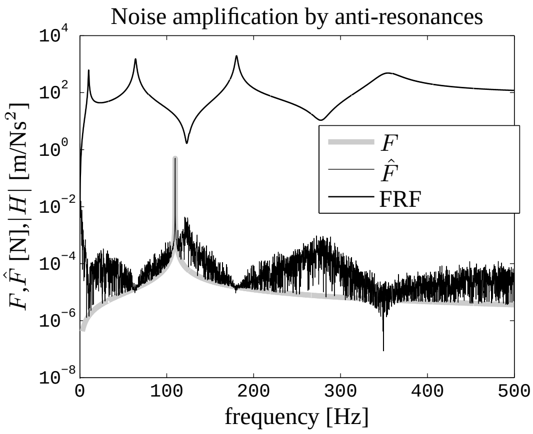

Figure 6: Noise amplification in anti-resonances

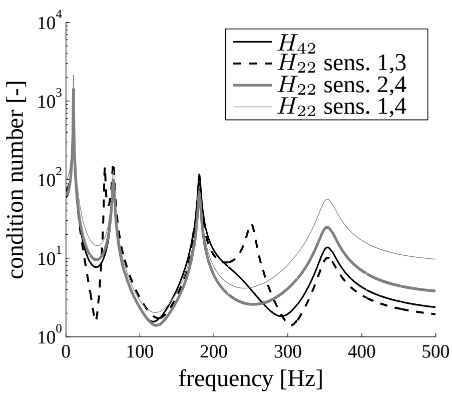

Figure 7: Condition of the FRM

Since the anti-resonance frequencies differ from sensor position to sensor position, it is often beneficial to use more sensors than forces to be reconstructed. So $m < n$ and $H_{1_{nm}}$ is no longer square. Using the pseudo-inverse $H_{1_{nm}}^{+}$ now gives a least-squares estimate of the solution to the over-determined system:

$$\hat{F}_n(\omega) = H^{+}_{1_{nm}}(\omega)A_m(\omega), \quad H^{+}_{1_{nm}} = [H^{*\mathrm{T}}_{1_{nm}} H_{1_{nm}}]^{-1} H^{*\mathrm{T}}_{1_{nm}} \tag{5}$$

where $H^{*\mathrm{T}}_{1_{nm}}$ (or: $H^{\mathrm{H}}_{1_{nm}}$) is the transpose of the complex conjugate of $H_{1_{nm}}$. Adding more sensor data not necessarily improves the force estimate since low quality sensor data can also be included. Figure 7 shows the condition number of the analytical FRM using all sensor data or a combination of two of them. The condition number of a FRM is the value of its highest singular value divided by the smallest. A high condition number indicates ill-conditioning since the reciprocal of a very small singular value will become large and cause amplification of small errors. Replacing very small singular values by zero is comparable with ignoring low quality sensor data and is applied in a regularization technique called Truncated Singular Value Decomposition (TSVD) [2].

NONLINEAR: CLAMPED-MAGNETICALLY SUPPORTED BEAM

The strongest nonlinearity in this project's benchmark, i.e. a car suspension, is caused by the bump-stop event, when the spring is fully compressed. Two repulsing magnets provide a non-contact approximation of this event. Moreover, this non-contact nonlinearity allows more accurate analytical modeling than e.g. a nonlinear spring. Therefore two cylindrical magnets are mounted as indicated in fig. 3. The specifications of the magnets are given in table 2. The magnets are mounted such that their separation at rest is about 12 mm; causing deflection of the beam tip.

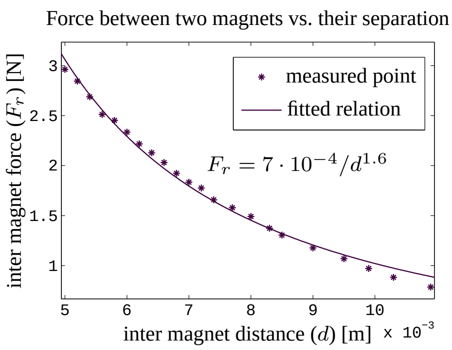

Figure 8: Fitted magnet characteristic

magnet dimensions		
diameter	14	[mm]
height	2.5	[mm]
weight	3	[gr]
material	neodymium	

Table 2: Magnets

The maximal excitation during the experiments was such that the minimal distance between the magnets was about 5 mm. The repulsive force (F_r) between the magnets versus their separation (d) was measured. The measured points are plotted in fig. 8 along with the fitted relation. A relation of the form $F_r(d) = C * d^b$ has been fitted because of the theoretical relation between rejecting magnetic monopoles, i.e. $F_r = C/d^2$ where C is a certain constant.

Numerical and experimental FRFs

The FRFs have been determined experimentally at different levels of excitation with three types of excitation: the impact hammer, white noise and a linear frequency sweep (chirp).

The nonlinear effects are most visible in the chirp based FRFs. Figure 9 shows such a FRF: the changes in the moduli around the eigenfrequencies clearly indicate nonlinearity.

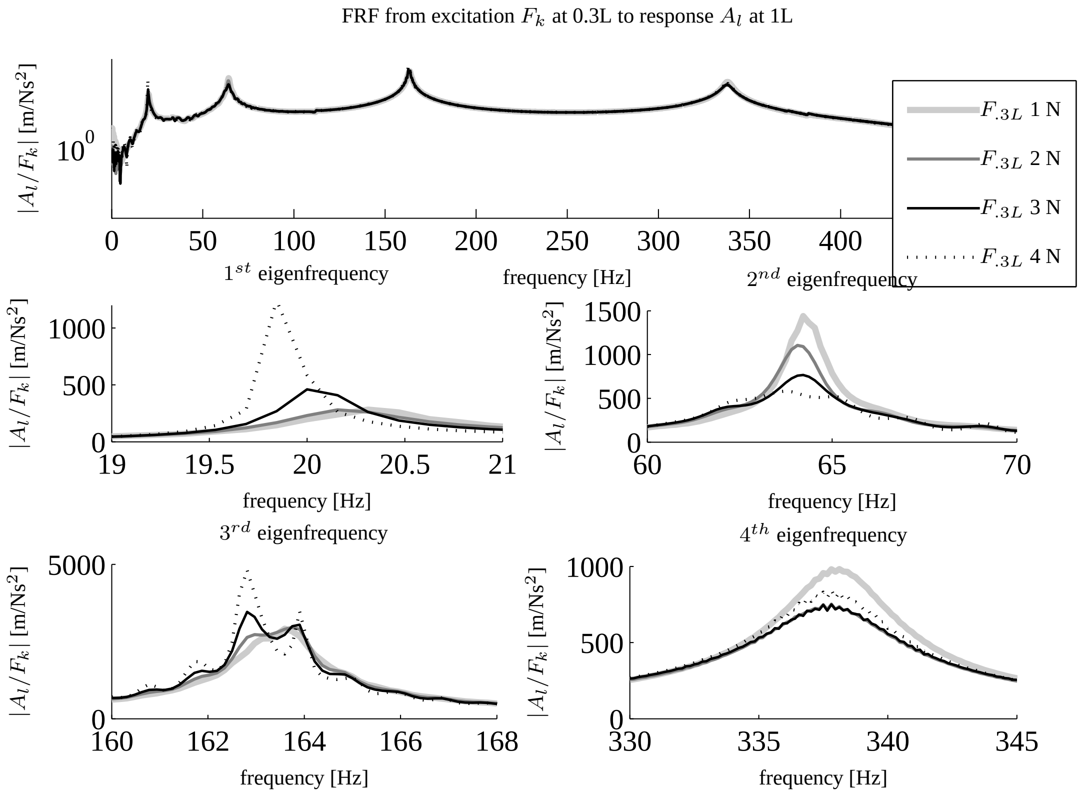

Figure 9: FRF from excitation at 0.3L to a sensor at 1L, with zooms

It is expected that one harmonic force at a certain excitation level can be predicted accurately using a matching transfer identified at the same level. However, the input force amplitude was not controlled, therefore the excitation signals from the force transducers are influenced by the shaker dynamics and their frequency spectrum shows no constant amplitude. In future experiments we will control the applied force instead of the input voltage to the shakers.

Force prediction

Figure 10 shows the reconstruction of a single harmonic force of 20 Hz at $0.3L$ with an amplitude of about 2 N, using the FRFs identified at the excitation levels 1 and 4 N. The influence of the chosen transfer is clear and a correct prediction should be possible with a matching FRF. The unwanted higher harmonics of the true excitation force due to the nonlinearity indicate the shaker dynamics' influence on the true excitation signal.

Since linear superposition of the responses to multiple forces is no longer valid, there is not *one* correct excitation level FRF to predict multiple harmonic forces, or excitation that is non-periodic with large differences in amplitude like road excitation data for vehicle durability testing. The next step in this research will be to examine this kind of excitation.

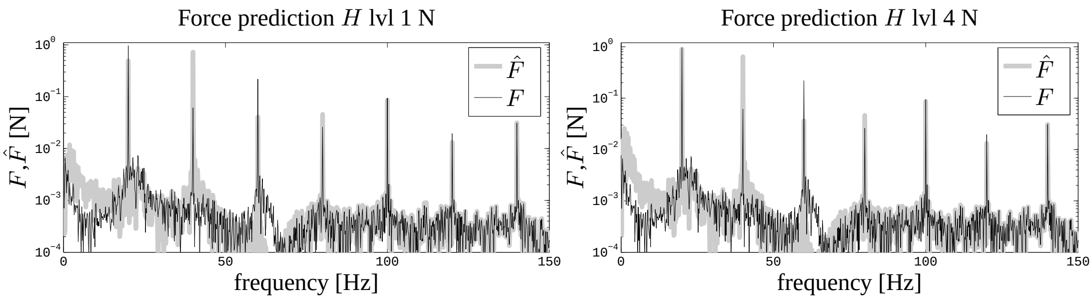

Figure 10: Force prediction using transfers H identified at different excitation levels

SUMMARY

To research the applicability and possible improvements of the direct force prediction approach when dealing with nonlinearities, a nonlinear demonstrator is studied both numerically and experimentally. However, to fully understand the effect of the direct force prediction approach in the frequency domain, first a linear demonstrator has been studied, both analytically and experimentally. The linear demonstrator consists of a clamped-free beam. The points of concern when using the inverse FRF in force prediction on the linear demonstrator have been illustrated. Subsequently the nonlinear behavior was invoked by placing a magnet on the aluminium beam and mounting a fixed, equal and repulsing magnet next to it. The magnets' nonlinear characteristic and its influence on the shape of the chirp-identified FRF, has also been illustrated. The effect of the nonlinearity on the force prediction of harmonic forces has been indicated. Further research on the nonlinear demonstrator will include the reconstruction on non-periodic forces, the applicability of the direct force prediction method in other domains and the use of the optimization approach.

REFERENCES

[1] B.-T. Wang, *Prediction of impact and harmonic forces acting on arbitrary structures: Theoretical formulation*, Mechanical Systems and Signal Processing, 16(6), (2002), 935–953.

[2] H. Inoue, J. Harrigan, S. Reid, *Review of inverse analysis for indirect measurement of impact force*, Applied Mechanics Reviews, 54(6), (2001), 503–524.

[3] T. Nordberg, *Time Domain Methods for Load Identification of Linear and Nonlinear Systems*, Phd thesis, Chalmers University of Technology (2004).

[4] C.-K. Ma, C.-C. Ho, *An inverse method for the estimation of input forces acting on non-linear structural systems*, Journal of Sound and Vibration, 275(3-5), (2004), 953–971.

[5] L. Meirovitch, *Fundamentals of Vibrations*, McGraw-Hill Higher Education, New York, 1 edn. (2001).

ACKNOWLEDGEMENTS

This work has been performed in the framework of the STW project INVERT, contract number TMR.5636. The support of STW is gratefully acknowledged.